

# Molecular Structure of Diphenylamine by Gas-Phase Electron Diffraction and Quantum Chemistry

V. A. Naumov\*, M. A. Tafipol'skii\*\*, A. V. Naumov\*, and S. Samdal\*\*\*

\* Arbuzov Institute of Organic and Physical Chemistry, Kazan Research Center,  
Russian Academy of Sciences, Kazan, Tatarstan, Russia

\*\* Institute of Inorganic Chemistry, Ruhr University, Bochum, Germany

\*\*\* University of Oslo, Oslo, Norway

Received January 24, 2004

**Abstract**—Geometric parameters of the diphenylamine molecule were determined by gas-phase electron diffraction and quantum-chemical calculations. By gas-phase electron diffraction, the molecule has an asymmetric structure with torsion angles about N–C bonds of  $-45.6(23)^\circ$  and  $173.4(46)^\circ$ , which agrees with RHF/6-31G\*\* calculations. Density functional theory (DFT) calculations at the B3LYP/6-31G\*\* level of theory lead to a  $C_2$  molecular conformation in the ground electronic state. The principal experimental geometric parameters are as follows: bond lengths: C–N 1.417(1), C–C<sub>av</sub> 1.403(1) Å; and bond angles: CNC  $123.9(5)^\circ$ , and NCC  $121.5^\circ$  (assumed) and  $116.4^\circ$ .

Proceeding with a systematic research into the structure of phenylphosphines [1–3], here we present the results of a structural study of diphenylamine (HNPH<sub>2</sub>). It is important to compare the conformations and structural parameters of mono-, di- and tri-phenylamines and -phosphines. The analysis of phenylphosphines is presented in [3]. The structure of gaseous diphenylamine has not been studied.

**Quantum-chemical calculations.** Geometry optimization of the diphenylamine molecule was performed by both semiempirical [4–9] and *ab initio* methods [8, 10–15]. In geometry optimization, the most important parameters that determine the conformation of this molecule are pyramidality of the N atom (measured by the sum of its bond angles) and torsion angles of phenyl groups relative to the C–N–C plane (Fig. 1). In view of the possibility of free rotation of phenyl groups and also the low barrier to inversion of the N atom, a number of possible conformations have been suggested for diphenylamine in the literature. Geometry optimization by semiempirical methods in different approximations (CNDO/2, INDO, MINDO/3, and MNDO) leads to a molecular conformation in which the N atom possesses a pyramidal coordination and phenyl groups have different torsion angles relative to the CNC plane. Therewith, the  $C^3C^2NC^8$  and  $C^9C^8NC^2$  torsion angles and differences between them depend remarkably on the method used [5]. By contrast, the AM1-optimized conformation [8] is propeller-like and has  $C_2$  sym-

metry with equal torsion angles ( $27.7^\circ$ ) and a planar coordination of bonds around the N atom. Moreover, Bredas *et al.* [8] have been the first who performed *ab initio* calculations of the diphenylamine molecule with the 3-21G basis set. The results of the latter calculation gave indirect evidence to show that the AM1 method is suitable for geometry optimization of diphenylamine and its analogs. Boyle [9] have optimized the geometry of diphenylamine molecule and some of its *ortho*-substituted analogs by the AM1 method and found that the global minimum corresponds to an asymmetric conformation with a pyramidal N atom and that the torsion angles of the phenyl rings relative to the CNC plane depend on the configuration of bonds around the N atom (planar or pyramidal). As follows from the results of *ab initio* calculations with the STO-3G and 6-31G basis sets [10], the most stable conformation possesses equal

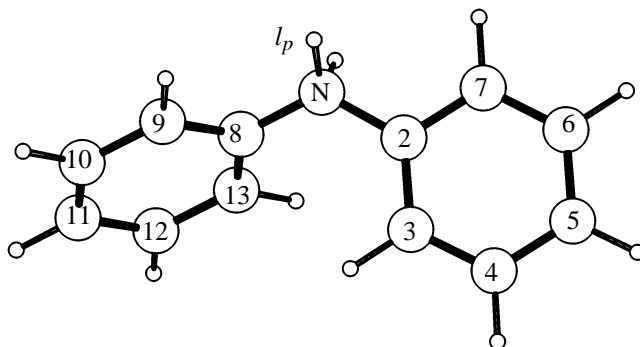


**Fig. 1.** Conformation of diphenylamine and atom numbering.

phenyl torsion angles (dihedral angles): 26.2° (RHF/STO-3G) and 29.5° (RHF/6-31G). The vibration frequencies calculated at these levels of theory confirmed that this conformation corresponds to the minimum on the potential energy surface of the diphenylamine molecule. Ito *et al.* [10] also optimized the geometries of two conformations of  $C_{2v}$  symmetry, the first being completely planar and the second having the phenyl rings perpendicular to the CNC plane, and one conformation of  $C_s$  symmetry, with phenyl rings rotated by 90° relative to the CNC plane. Vibration frequencies were calculated to show that the optimized geometries corresponding to the above models are not local minima but transition states on the potential energy surface of diphenylamine. In [11], the geometry of the molecular model of  $C_1$  symmetry was optimized using the 6-31G\* basis set augmented with polarization  $d$  functions on the C and N atoms. The dihedral angles for the resulting minima are markedly different: 13.9° and 48.8°. The H atom deviates from the CNC plane by 26.3°. Based on calculated vibration frequencies, Choi and Kertesz [11] assigned the IR and Raman spectra of diphenylamine. The conclusion of that the N atom has a pyramidal coordination and the phenyl rings are non-equivalent agrees with the results of the experimental data of Boogaarts *et al.* [12] who also performed *ab initio* calculations with the even larger 6-31G\*\* basis set (including polarization  $p$  functions on H atoms). Similar results were also obtained for torsion angles (14.7° and 44.5°) and deviation of the H atom from the CNC plane (20.8°). It is interesting to note that the geometry of the first electronically excited state (singlet), obtained in [12], correspond to a molecular conformation of  $C_2$  symmetry with a planar coordination of bonds around the N atom. The nonequivalent orientation of the rings in the ground electronic state of diphenylamine is disputed by Tretiakov and Cable [13] who concluded that the vibrationally allowed electronic spectra of diphenylamine and three its deuterated analogs, obtained in expanded supersonic jet with resonance-enhanced two-photon ionization, better agree with a  $C_2$  molecular geometry both in the ground and first excited singlet electronic state. The same authors note that the HF/6-31G\*\*-optimized  $C_2$  model of diphenylamine corresponds to a transition state on the potential energy surface, rather than to a local minimum (one imaginary frequency was revealed). Therewith, the energy gap between the  $C_1$  and  $C_2$  conformations is small (0.04 kcal mol<sup>-1</sup>).

Thus, from on the above calculation results one or another model for the free diphenylamine molecule is difficult to choose unambiguously. More precise calculations give preference for the propeller-like conformation, but a higher symmetry model ( $C_2$ )

cannot be ruled out. Therewith, one should note that the cited calculations all did not include electron correlation. Recently Xiao *et al.* [14] reported the geometry optimization with inclusion of electron correlation at the MP2/6-31G\* level of theory. The phenyl rings in the resulting diphenylamine conformation are rotated by different angles relative to the CNC plane (9.6° and 46.8°), and the N atom has a pyramidal coordination. Unfortunately, the referees did not perform MP2/6-31G\* calculations of vibration frequencies. At the same time, Budyka and Zyubina [15], based on the geometry optimized by DFT B3LYP/6-31G\* calculations [16, 17], showed that the ground electronic state of the molecule is described by a symmetric model ( $C_2$ ) with a planar N atom and the phenyl rings rotated by the same angle relative to the CNC plane (24.8°).

In the present work we performed full geometry optimization and calculated vibration frequencies for optimized diphenylamine structures, by the DFT method with the B3LYP functional and 6-31G\*\* [18] and cc-pVDZ [19] basis sets. Such calculations are widely used for geometry optimization and vibrational analysis of organic molecules. To find out how the calculation results depend on the theoretical basis, we also performed Hartree-Fock calculations with various basis sets: ST-3G, 3-21G, 6-31G, 6-31G\*, 6-31G\*\*, 6-311G\*\*, and 6-311++G\*\*. All calculations were performed using the GAUSSIAN program [18]. In the calculation of the geometry and vibration spectra by the B3LYP method we used a tight convergence criterion and an ultrafine integration grid. This approach is required for more correct low vibration frequencies.

Our results provide evidence to show that the optimized geometry of diphenylamine is basis-dependent. Thus, according to RHF/STO-3G calculations, the  $C_2$  model corresponds not to a local minimum but to a transition state (one imaginary frequency in the spectrum), whereas RHF/3-21 and RHF/6-31G calculations result on a local minimum for the  $C_2$  model (no imaginary frequencies were revealed). More extended basis sets (6-31G\*, 6-31G\*\*, 6-311G\*\*, and 6-311++G\*\*) revealed one imaginary frequency in the spectrum for  $C_2$  symmetry (in the region 30–60 cm<sup>-1</sup>). It is interesting to note that inclusion of electron correlation (B3LYP) results in that both in the 6-31G\*\* basis set and in the more extended cc-pVDZ basis set the molecular model of  $C_2$  symmetry corresponds to a local minimum. Therewith, both calculations give very close lowest vibration frequencies (cm<sup>-1</sup>): 36, 55, and 109 (B3LYP/6-31G\*\*) and 32, 50, and 108 (B3LYP-cc-pVDZ). Variation in convergence criteria and more correct integration grids lead (B3LYP 6-31G\*\*) to similar

**Table 1.** Comparison of the calculated and experimental geometric parameters of diphenylamine and aniline (Å, deg)

Parameter	H <sub>2</sub> NPh			HNPh <sub>2</sub> (C <sub>1</sub> symmetry)			HNPh <sub>2</sub> (C <sub>2</sub> symmetry)				
	experiment	HF/6-6-31G*	HF/6-31G**	HF/6-31G*	HF/6-31G**	experiment, <sup>a</sup> <i>r<sub>a</sub></i>	b3lyp/6-31G**	b3lyp/6cc-pVDZ	HF/6-31G**	HF/6-31G**	experiment, <sup>a</sup> <i>r<sub>a</sub></i>
N–C <sup>2</sup>	1.402 (3)	1.397	1.401	1.401	1.399	1.417 (1)	1.399	1.399	1.396	1.396	1.408 (1)
N–C <sup>8</sup>	–	–	–	1.402	1.400	1.417	1.399	1.399	1.396	1.396	1.408
C <sup>2</sup> –C <sup>3</sup>	1.397 (3)	1.393	1.405	1.394	1.394	1.412	1.406	1.409	1.393	1.392	1.416
C <sup>3</sup> –C <sup>4</sup>	1.394 (4)	1.383	1.393	1.383	1.383	1.402	1.394	1.396	1.384	1.384	1.400
C <sup>4</sup> –C <sup>5</sup>	1.386 (4)	1.386	1.397	1.387	1.386	1.404	1.395	1.399	1.385	1.384	1.405
C <sup>5</sup> –C <sup>6</sup>	1.386 (4)	1.386	1.397	1.384	1.384	1.404	1.397	1.399	1.385	1.384	1.404
C <sup>6</sup> –C <sup>7</sup>	1.394 (4)	1.383	1.393	1.385	1.385	1.402	1.391	1.391	1.383	1.382	1.403
C <sup>7</sup> –C <sup>2</sup>	1.397 (3)	1.393	1.405	1.391	1.391	1.412	1.407	1.410	1.394	1.393	1.415
C <sup>8</sup> –C <sup>9</sup>	–	–	–	1.395	1.395	1.412	1.407	1.410	1.394	1.393	1.416
C <sup>9</sup> –C <sup>10</sup>	–	–	–	1.381	1.381	1.402	1.391	1.394	1.383	1.382	1.400
C <sup>10</sup> –C <sup>11</sup>	–	–	–	1.387	1.386	1.404	1.397	1.399	1.385	1.384	1.405
C <sup>11</sup> –C <sup>12</sup>	–	–	–	1.383	1.383	1.404	1.395	1.398	1.385	1.384	1.404
C <sup>12</sup> –C <sup>13</sup>	–	–	–	1.386	1.386	1.402	1.394	1.396	1.384	1.384	1.403
C <sup>13</sup> –C <sup>8</sup>	–	–	–	1.391	1.393	1.412	1.406	1.409	1.393	1.392	1.416
C–C <sub>av</sub> <sup>b</sup>	1.390	–	–	1.387	1.387	1.403	–	–	–	–	1.403
C–H	–	1.076	1.087	1.076	1.076	1.079 (2)	1.086	1.092	1.076	1.075	1.079 (2)
N–H	–	0.997	1.013	0.995	0.993	0.995 <sup>c</sup>	1.009	1.012	0.994	0.992	1.009 <sup>c</sup>
NC <sup>2</sup> C <sup>3</sup>	120.6	120.6	120.7	121.3	121.5	121.5 <sup>c</sup>	123.1	123.3	122.6	122.5	117.9 (3)
NC <sup>8</sup> C <sup>9</sup>	–	–	–	117.9	118.0	116.4 (6)	118.3	118.2	118.8	118.7	117.9
C <sup>2</sup> C <sup>3</sup> C <sup>4</sup>	120.4	120.4	120.5	120.2	120.2	120.3 <sup>c</sup>	120.1	120.2	120.1	120.2	120.7 <sup>c</sup>
C <sup>3</sup> C <sup>4</sup> C <sup>5</sup>	120.9	120.9	120.8	120.9	120.9	120.7 <sup>c</sup>	121.1	121.2	121.1	121.1	120.6 <sup>c</sup>
C <sup>4</sup> C <sup>5</sup> C <sup>6</sup>	118.8	118.8	118.9	119.0	119.0	119.0 <sup>c</sup>	118.9	118.9	118.8	118.8	118.9 <sup>c</sup>
C <sup>5</sup> C <sup>6</sup> C <sup>7</sup>	120.9	120.9	120.8	120.5	120.6	120.8 <sup>d</sup>	120.6	120.6	120.6	120.6	121.1 <sup>d</sup>
C <sup>6</sup> C <sup>7</sup> C <sup>2</sup>	120.4	120.4	120.5	120.6	120.6	120.2 <sup>d</sup>	120.7	120.8	120.6	120.6	120.1 <sup>d</sup>
C <sup>7</sup> C <sup>2</sup> C <sup>3</sup>	118.7 <sup>e</sup>	118.7	118.6	118.8	118.8	119.0 <sup>d</sup>	118.6	118.4	118.7	118.7	118.6 <sup>d</sup>
CNC	110.6	–	–	126.6	126.9	123.5 (5)	129.8	130.2	128.5	128.4	125.5 (4)
HNC <sub>av</sub>	113.1 (1)	–	–	114.3	114.7	114.3 <sup>d</sup>	115.1	114.9	115.8	115.8	117.0 <sup>c</sup>
τ(C <sup>2</sup> NC <sup>8</sup> C <sup>9</sup> )	–	–	–	167.3	165.7	173.3 (46)	157.9	158.3	152.6	152.2	144.8 (10)
τ(C <sup>8</sup> NC <sup>2</sup> C <sup>3</sup> )	37.5 (2) <sup>f</sup>	–	–	–48.8	–46.5	–45.6 (23)	–24.9	–24.3	–30.0	–30.3	144.8
<i>l<sub>p</sub></i> (NC <sup>2</sup> C <sup>3</sup> )	90.0	–	–	56.0	54.2	62.0	–	–	–	–	–
<i>l<sub>p</sub></i> (NC <sup>8</sup> C <sup>9</sup> )	–	–	–	62.5	64.2	65.8	–	–	–	–	–
<i>R</i> factor, %	–	–	–	–	–	2.91	–	–	–	–	4.12

<sup>a</sup> Parenthesized values are standard deviations. <sup>b</sup> Without inclusion of C<sub>ipso</sub>–C distances. <sup>c</sup> Fixed parameters. <sup>d</sup> Dependent parameters.

<sup>e</sup> HNH bond angle. <sup>f</sup> Angle between the phenyl and HNH planes.

results (cm<sup>–1</sup>): 34, 55, and 108. It is also important to note that the DFT B3LYP/6-31G\* calculation starting from the asymmetric model (C<sub>1</sub>) lead to a C<sub>2</sub> molecular model.

These findings point to the fact that the effects of electron correlation and basis extension are mutually compensating. We also optimized (B3LYP/6-31G\*\*) molecular models of C<sub>2v</sub> (all atoms are in the same plane) and C<sub>s</sub> symmetry (phenyl rings are rotated by the same angle but in opposite sides relative to the CNC plane). As follows from the calculation results,

the C<sub>2v</sub> model corresponds to a transition state (one imaginary vibration frequency) between two conformations of C<sub>2</sub> symmetry, because the vibration at this imaginary frequency (near 95 cm<sup>–1</sup>) describes phenyl ring torsion about the C–N bond and leads to a conformation of C<sub>2</sub> symmetry. Therewith, the energy gap between the C<sub>2</sub> and C<sub>2v</sub> conformations is (without inclusion of zero-point vibrations) is 2.6 kcal mol<sup>–1</sup>. Calculation with the starting diphenylamine geometry, corresponding to the C<sub>2</sub> molecular model, leads to a C<sub>2v</sub> molecular model. Table 1 compares the geo-

metrical parameters of diphenylamine, obtained at various levels of theory.

**Normal coordinate analysis.** The IR spectra of diphenylamine in the gas phase are lacking, but those in solution ( $\text{CCl}_4$ ), liquid, and crystal are available [7, 20–24]. The crystal spectrum is more complicated and in general is similar to the spectra in solution and liquid (melt at 367 K).

The vibration spectra of diphenylamine have been considered in [7, 11–13, 20–22]. Thus, Sett *et al.* [7] preliminary assigned experimental IR and Raman frequencies in terms of  $C_{2v}$  symmetry, but did not calculate frequencies. Choi and Kertesz [11] performed full assignment of vibration frequencies on the basis of RHF/6-31G\* *ab initio* calculations and found that the experimental IR and Raman intensities are well described by an asymmetric molecular model ( $C_1$ ). The lowest vibration frequencies were assigned in [11] on the basis of HF/6-31G\*\* results. Srivastava and Kumar [20] empirically interpreted their observed IR frequencies in terms of the  $C_{2v}$  molecular model. It is interesting to note that Kostic *et al.* [21] assigned the IR spectra of diphenylamine on the basis of the results of solution of the inverse vibrational task in terms of valence optical theory for the  $C_2$  molecular model. The vibration frequencies and intensities obtained in this work on the basis of calculated empirical force constants and electrooptical parameters are in agreement with experiment. Cochet *et al.* [22] assigned the IR and Raman (solid state) spectra in the region of conformational vibrations ( $200\text{--}1000\text{ cm}^{-1}$ ) on the basis of valence force field calculations.

Our normal coordinate analysis was performed on the basis of harmonic force fields calculated at the RHF/6-31G\*\* ( $C_1$  symmetry) and B3LYP/6-31G\*\* ( $C_2$  symmetry) levels of theory. The calculations were performed using a computer program [25] modified by one of us. The assignment of vibration frequencies is presented in Table 2. Taking into account that the asymmetric molecular conformation obtained at the RHF/6-31G\*\* level of theory is very close in energy to the symmetric structure ( $C_2$ ), the assignment of frequencies was limited to this calculation that is qualitatively is very similar to the assignment of frequencies at the B3LYP/6-31G\*\* level of theory. The calculated frequencies (after scaling) and IR intensities fit both experimental [7, 20–24] and calculated by other authors [11].

As follows from the experience, calculated harmonic force fields allow reliable estimation of the mean vibration amplitudes  $u_{ij}$ . Precision of the estimates can be tested from their comparison with well-known theoretical  $u_{ij}$  values for the C–C, C–H, C...C,

and C...H distances in the benzene ring (a kind of internal reference) and with experimental IR frequencies. This is especially important for nonbonded C...C, C...H and H...H distances between the  $C^{2-7}$  and  $C^{8-13}$  atoms of the phenyl rings. Table 3 shows the RHF/6-31G\*\* vibration amplitudes some of which were refined in the structural analysis. Note that the vibration amplitudes calculated at RHF/6-31G\*\* and RHF/6-31G\* levels of theory are similar.

**Structural analysis and discussion.** The geometry of diphenylamine is described by the following independent structural parameters: N–C, C–C, N–H, and C–H bond lengths, CNC, NCC, and CNH bond angles, and phenyl CCC and CCH angles. The molecular conformation is determined by the  $C^8NC^2C^3$  and  $C^2NC^8C^9$  torsion angles (Fig. 1). Note that the N–H bond is almost in the  $C^2\cdots C^7$  phenyl plane (the  $HNC^2C^3$  torsion angle is  $157^\circ$  by both HF calculations). The closest contacts between the phenyl rings are  $C^2\cdots C^{13}$  ( $2.98\text{ \AA}$ ) and  $C^3\cdots C^8$  ( $3.11\text{ \AA}$ ). The corresponding torsion angles  $C^2NC^8C^{13}$  and  $C^8NC^2C^3$  are  $-15^\circ$  and  $-47^\circ$ . Obviously, all C–C and C–N distances are difficult to determine because of their closeness and strong mutual correlations. The same is true of CCC bond angles. Nevertheless we refined independent bond angles in the general cycle of structural analysis. It was found they have changed only slightly, within standard deviations ( $\sim 1^\circ$ ), but, as would be expected, strong correlations between them were observed. C–N bond distances were refined independently. The parameter  $\Delta(\text{CN})$ , i.e. the theoretical difference between  $r(C^2\cdots C^3)$  and  $r(\text{C–N})$ , has increased by  $0.0016\text{ \AA}$ . Therewith, the *R* factor has not changed (Table 1). Therefore, we refined C–C and C–N distances as a single parameter taking account for the differences  $\Delta(\text{C–C})$  and  $\Delta(\text{C–N})$  between the “base” parameter  $C^2\cdots C^3$  and remaining  $C^i\cdots C^j$  distances, including C–N. The  $\Delta(\text{C–C})$  and  $\Delta(\text{C–N})$  differences were fixed at values calculated at the RHF/6-31G\*\* level of theory. Both calculations showed that the  $C_{ipso}\text{--C}$  distances are longer than other C–C bonds (by  $0.011\text{--}0.012\text{ \AA}$ ). The reasons for this elongation will be discussed below. Both calculations give  $\text{CC}_{ipso}\text{C}$  and opposite CCC angles smaller  $120^\circ$ . As follows from analysis of the calculated geometry of diphenylamine, the phenyl rings with a sufficient confidence can be described by  $C_s$  symmetry. Following Domenicano [26], let us label the  $\text{CC}_{ipso}\text{C}$  and  $C_{ipso}\text{CC}$  bond angles  $\alpha$  and  $\beta$ , respectively, and the next two angles  $\gamma$  and  $\delta$ . In the structural analysis we used as independent parameters the  $\beta$ ,  $\gamma$  and  $\delta$  bond angles for both rings ( $120.3^\circ$ ,  $120.72^\circ$  and  $119.^\circ$ , respectively) and fixed them. The  $\text{NC}^2\text{C}^3$  ( $121.5^\circ$ ) and  $\text{NC}^8\text{C}^9$  ( $118.0^\circ$ ) bond angles do not lie

**Table 2.** Results of normal coordinate analysis of HNPh<sub>2</sub><sup>a</sup>

HF/6-31G**			Experiment [24]		
$\omega$ , cm <sup>-1</sup>	$\omega^*$ , cm <sup>-1</sup>	PED, %	liquid	solvent, 300 K	crystal, 77 K
3882	3407 (27)	99 $\nu_{\text{NH}}$	3390 (7)	3433 s	3415 m, 3395 s
3386	3086 (7)	88 $\nu_{\text{CH}}$	—	3091 s	3090 w
3378	3079 (6)	83 $\nu_{\text{CH}}$	—	—	—
3370	3072 (18)	73 $\nu_{\text{CH}}$	—	3063 s	3075 w
3369	3070 (67)	82 $\nu_{\text{CH}}$	—	—	—
3354	3057 (50)	96 $\nu_{\text{CH}}$	3049 (6)	3046 s	3040 w
3354	3057 (25)	89 $\nu_{\text{CH}}$	—	—	—
3343	3047	87 $\nu_{\text{CH}}$	—	—	—
3342	3047	87 $\nu_{\text{CH}}$	—	—	—
3334	3039 (9)	87 $\nu_{\text{CH}}$	—	3019 s	3020 w
3333	3038 (13)	86 $\nu_{\text{CH}}$	—	—	3015 w
1812	1611 (10)	52 $\nu_{\text{CC}}$	—	1600 sh	1618 sh
1799	1600 (270)	52 $\nu_{\text{CC}}$	1595 (10)	1594 m	1608 w
1790	1593 (6)	48 $\nu_{\text{CC}}$ + 10 $\alpha_{\text{CNH}}$	—	—	1597 sh
1784	1586 (12)	62 $\nu_{\text{CC}}$	—	—	1588 s
1691	1512 (208)	17 $\nu_{\text{CN}}$ + 31 $\nu_{\text{CNH}}$	—	—	1528 s
1667	1494 (14)	20 $\nu_{\text{CC}}$ + 55 $\alpha_{\text{CCH}}$	—	1508 w	1517 s
1659	1488 (132)	22 $\nu_{\text{CC}}$ + 47 $\alpha_{\text{CCH}}$	1492 (10)	1494 w	1501 s, 1488 w, 1482 w
1624	1457 (7)	19 $\nu_{\text{CC}}$ + 44 $\alpha_{\text{CCH}}$	1460 (6)	1459 s	1464 s, 1460 sh
1575	1413 (26)	17 $\nu_{\text{CNH}}$ + 46 $\alpha_{\text{CCH}}$	1418 (8)	1415 s	1423 s, 1418 sh
1479	1331	82 $\alpha_{\text{CCH}}$	—	1337 m	1346 sh, 1338 m
1455	1305 (41)	57 $\alpha_{\text{CCH}}$	1311 (10)	—	1329 s, 1312 m, 1301 w
1420	1256 (238)	55 $\nu_{\text{CN}}$	1245 (7)	1243 s	1245 m
1351	1204 (1)	12 $\nu_{\text{CN}}$ + 27 $\nu_{\text{CC}}$ + 31 $\alpha_{\text{CCH}}$	1221 (2)	1215 w	1226 m
1325	1181 (6)	21 $\nu_{\text{CC}}$ + 26 $\nu_{\text{CN}}$ + 20 $\alpha_{\text{CCH}}$	—	—	1187 vw
1313	1176 (2)	25 $\nu_{\text{CC}}$ + 49 $\alpha_{\text{CCH}}$	1174 (7)	1177 sh	1182 w
1296	1162	13 $\nu_{\text{CC}}$ + 60 $\alpha_{\text{CCH}}$	—	1171 m	1177 m
1293	1160 (9)	11 $\nu_{\text{CC}}$ + 64 $\alpha_{\text{CCH}}$	1155 (4)	1153 s	1161 m, 1149 m
1216	1082 (4)	67 $\nu_{\text{CC}}$ + 12 $\alpha_{\text{CCH}}$	—	—	1089 m
1198	1064 (5)	71 $\nu_{\text{CC}}$ + 13 $\alpha_{\text{CCH}}$	1081 (4)	1080 s	1086 m
1191	1063 (7)	67 $\nu_{\text{CC}}$	1074 (4)	1072 s	1075 m
1185	1059 (5)	58 $\nu_{\text{CC}}$	—	—	1071 sh
1128	1009	48 $\nu_{\text{CC}}$	1028 (6)	1028 m	1031 m
1130	1007	40 $\nu_{\text{CC}}$	—	—	1026 w, 1023 sh
1116	1004 (1)	68 $\gamma_{\text{CH}}$	—	—	—
1113	1002	67 $\gamma_{\text{CH}}$ + 11 $\tau_{\text{CC}}$	996 (4)	999 s	996 m
1097	987	58 $\gamma_{\text{CH}}$	—	—	—
1094	985 (1)	70 $\gamma_{\text{CH}}$	—	—	992 w
1085	971	24 $\nu_{\text{CC}}$ + 44 $\alpha_{\text{CCC}}$	—	—	980 w
1084	968 (3)	34 $\nu_{\text{CC}}$ + 33 $\alpha_{\text{CCC}}$	—	969 w	973 vw, 962 vw
1020	917 (13)	66 $\gamma_{\text{CH}}$	—	954 w	882 m
1008	907 (10)	70 $\gamma_{\text{CH}}$	874 (6)	875 m	878 s
955	850	10 $\nu_{\text{CN}}$ + 15 $\nu_{\text{CC}}$ + 35 $\gamma_{\text{CH}}$	—	—	—
945	850 (3)	73 $\gamma_{\text{CH}}$	822 (1)	—	850 w
933	837 (3)	13 $\nu_{\text{CC}}$ + 10 $\nu_{\text{CN}}$ + 42 $\gamma_{\text{CH}}$	—	827 sh	841 w
899	804 (123)	14 $\nu_{\text{CC}}$ + 15 $\gamma_{\text{CN}}$ + 30 $\gamma_{\text{CC}}$	—	817 v.s	805 w, 798 w
845	761 (16)	60 $\gamma_{\text{CH}}$ + 19 $\gamma_{\text{CC}}$	—	—	759 w
834	747 (10)	51 $\gamma_{\text{CH}}$	746 (10)	745 v.s	752 v.s, 746 v.s

**Table 2.** (Contd.)

HF/6-31G**			Experiment [24]		
$\omega$ , cm <sup>-1</sup>	$\omega^*$ , cm <sup>-1</sup>	PED, %	liquid	solvent, 300 K	crystal, 77 K
778	700 (26)	34 $\gamma_{CH}$ + 17 $\gamma_{CC}$ + 34 $\gamma_{CH}$	—	695 sh	703 v.s
772	695 (7)	50 $\gamma_{CH}$ + 23 $\tau_{CC}$	690 (10)	689 v.s	689 v.s
679	610 (2)	57 $\alpha_{CCC}$	—	617 v.s	612 m
675	607 (2)	54 $\alpha_{CCC}$	—	—	—
623	559 (7)	53 $\alpha_{CCC}$ + 10 $\alpha_{NCC}$	—	569 s	565 w
564	507 (2)	52 $\gamma_{CC}$	—	498 m	505 m
544	490	36 $\gamma_{CH}$ + 10 $\tau_{CC}$ + 19 $\gamma_{CC}$	—	487 sh	491 m
461	415	31 $\gamma_{CH}$ + 50 $\tau_{CC}$	—	—	430 m
457	411 (30)	29 $\gamma_{CH}$ + 51 $\tau_{CC}$	—	412 s	415 w
394	353 (10)	30 $\alpha_{NCC}$ + 18 $\alpha_{CCC}$	—	406 s	406 w
Raman spectra [7]			Solvent	Solvent	Crystal
335	298 (2)	25 $\nu_{CN}$ + 29 $\tau_{CN,CC}$	333 w	—	—
315	283 (10)	20 $\gamma_{NC}$ + 43 $\tau_{CN}$	—	—	305 m
251	226 (5)	37 $\tau_{CC}$ + 10 $\gamma_{CH}$	238 sh	—	241 m
227	204 (3)	39 $\tau_{NC}$ + 33 $\tau_{CC}$	218 w	217 w	221 m
104	94 (1)	20 $\alpha_{CNC}$ + 20 $\tau_{CC}$ + 19 $\tau_{CN}$	138 w	125 m	130 m
47	43 (1)	14 $\alpha_{CNC}$ + 65 $\tau_{CN}$	—	—	—
26	24 (2)	14 $\gamma_{CC}$ + 61 $\tau_{CN}$	—	—	—

<sup>a</sup> Parenthesized values are intensities. ( $\omega$ ,  $\omega^*$ ) Unscaled and scaled theoretical frequencies, respectively; ( $\nu$ ,  $\alpha$ ,  $\gamma$ , and  $\tau$ ) Stretching, in-plane, out-of-plane, and torsion vibrations, respectively.

on the  $C_2$  symmetry axes that pass through the  $C^2$  and  $C^5$  atoms in the first ring and through the  $C^8$  and  $C^{11}$  atoms in the second ring. When refining the  $NC^2C^3$  bond angle we found that it strongly correlates with the  $NC^8C^9$  bond angle [87]  $\tau(C^2NC^8C^9)$  [88],  $\tau(C^3C^2NC^8)$  [74], and amplitudes  $u(C\cdots C)$  and  $u(N\cdots C)$  of the type 1,3 (2.4 Å) and  $u(C\cdots C)$  of the type 1,4

(3.8 Å). Therewith, the  $NC^3C^3$  bond angle remained practically unchanged (121.3°). For this reason, the  $NC^2C^3$  bond angle was fixed. The selected set of independent parameters allowed us to exclude correlations, as seen from the correlation matrix given below ( $\times 10^2$ ; in parentheses for the amplitudes  $u$  we show groups of distances).

$r(C-C, C-N)$	100												
$r(C-H)$	7	100											
$\angle CNC$	-32	24	100										
$\angle C^9C^8C^1$	-35	18	3	100									
$\angle (C^8NC^2C^3)$	-1	-7	62	-58	100								
$\tau(C^2NC^8C^9)$	-14	-15	-6	52	-36	100							
$u(C-N, C-C)$	-18	-6	7	2	3	-7	100						
$u(N-H, C-H)$	18	10	-7	-6	-2	-5	-11	100					
$u(N\cdots C, C\cdots C)$ (2.5 Å)	-16	16	-8	69	-51	33	33	-5	100				
$u(N\cdots C, C\cdots C)$ (3.8 Å)	-25	-13	11	34	-6	24	15	-6	20	100			
$u(C\cdots C)$ (4.3 Å)	7	-11	-8	-24	17	-23	0	1	-16	-7	100		
$u(C\cdots C)$ (2.8 Å)	-9	6	-14	11	-9	11	22	5	0	12	3	100	
$u(C\cdots H)$ (2.15 Å)	28	-4	-3	-4	0	6	-17	2	17	-6	1	-33	100

The structural analysis was conducted on the basis of molecular intensity curves  $sM(s)$  (Fig. 2). As follows from the assignment of peaks on the experi-

mental radial distribution curve (Fig. 3), there is no need in refining vibration amplitudes for long  $C\cdots C$  distances between the phenyl rings. The final results

**Table 3.** Principal experimental and calculated mean vibration amplitudes

Parameter	$R_{ij}$ , Å	Calculation	Experiment	Parameter	$r_{ij}$ , Å	Calculation
N–C	1.40	0.049	0.050 (1) <sup>a</sup>	C <sup>6</sup> ...C <sup>8</sup>	4.84	0.164
C–C	1.39	0.047	0.046	C <sup>4</sup> ...C <sup>9</sup>	5.74	0.218
N...C <sup>3</sup>	2.44	0.063	0.063 (1) <sup>b</sup>	C <sup>5</sup> ...C <sup>9</sup>	6.47	0.136
N...C <sup>7</sup>	2.44	0.068	0.068	C <sup>6</sup> ...C <sup>9</sup>	6.06	0.136
N...C <sup>13</sup>	2.50	0.064	0.064	C <sup>7</sup> ...C <sup>9</sup>	4.77	0.159
C <sup>2</sup> ...C <sup>4</sup>	2.41	0.056	0.055	C <sup>2</sup> ...C <sup>10</sup>	4.90	0.094
C <sup>2</sup> ...C <sup>8</sup>	2.55	0.082	0.082	C <sup>3</sup> ...C <sup>10</sup>	5.37	0.265
N...C <sup>4</sup>	3.70	0.064	0.057 (2) <sup>c</sup>	C <sup>4</sup> ...C <sup>10</sup>	6.73	0.249
N...C <sup>6</sup>	3.73	0.067	0.068	C <sup>5</sup> ...C <sup>10</sup>	7.57	0.162
N...C <sup>10</sup>	3.71	0.064	0.058	C <sup>6</sup> ...C <sup>10</sup>	7.27	0.191
C <sup>7</sup> ...C <sup>8</sup>	3.63	0.176	0.170	C <sup>7</sup> ...C <sup>10</sup>	6.00	0.210
C <sup>2</sup> ...C <sup>9</sup>	3.72	0.093	0.087	C <sup>2</sup> ...C <sup>11</sup>	5.19	0.119
N...C <sup>5</sup>	4.20	0.063	0.068 (5) <sup>d</sup>	C <sup>3</sup> ...C <sup>11</sup>	5.43	0.258
N...C <sup>11</sup>	4.25	0.066	0.069	C <sup>4</sup> ...C <sup>11</sup>	6.70	0.254
C <sup>4</sup> ...C <sup>8</sup>	4.45	0.133	0.136	C <sup>5</sup> ...C <sup>11</sup>	7.62	0.246
C <sup>2</sup> ...C <sup>12</sup>	4.39	0.156	0.159	C <sup>6</sup> ...C <sup>11</sup>	7.44	0.311
C <sup>3</sup> ...C <sup>12</sup>	4.49	0.229	0.232	C <sup>7</sup> ...C <sup>11</sup>	6.32	0.297
C <sup>4</sup> ...C <sup>13</sup>	4.26	0.223	0.226	C <sup>4</sup> ...C <sup>12</sup>	5.64	0.256
C <sup>3</sup> ...C <sup>9</sup>	4.36	0.237	0.240	C <sup>5</sup> ...C <sup>12</sup>	6.44	0.334
C <sup>7</sup> ...C <sup>13</sup>	4.14	0.349	0.352	C <sup>6</sup> ...C <sup>12</sup>	6.47	0.410
C <sup>2</sup> ...C <sup>5</sup>	2.80	0.064	0.065 (2) <sup>e</sup>	C <sup>7</sup> ...C <sup>12</sup>	5.52	0.369
C <sup>3</sup> ...C <sup>8</sup>	3.11	0.151	0.151	C <sup>5</sup> ...C <sup>13</sup>	5.14	0.311
C <sup>2</sup> ...C <sup>13</sup>	2.98	0.167	0.168	C <sup>6</sup> ...C <sup>13</sup>	5.02	0.377
C <sup>3</sup> ...C <sup>13</sup>	3.07	0.193	0.194			
C...H	2.15	0.099	0.101			

a–e Criteria for group refinement.

of the structural analysis are presented in Tables 1 and 3. In essence, the diffraction pattern of diphenylamine is defined by the NPh<sub>2</sub> moiety. We performed structural analysis of diphenylamine with a symmetric NPh<sub>2</sub> fragment (C<sub>2</sub> or C<sub>s</sub>). The fit of the calculated molecular intensity curves  $sM(s)$  to experimental proved to be worse then for the structure predicted by theoretical calculations at different levels of theory (Table 1). The torsion angles around the N–C bond for the C<sub>2</sub> model of the NPh<sub>2</sub> fragment are 145° (*R* factor 4.12, ∠CNC 125°, Table 1) and for the C<sub>s</sub> model, C–N are ±145° (*R* factor 3.53, ∠CNC 125°).

In [26, 27], abundant experimental evidence on the effect of a heteroatom on the structure of the phenyl rings is presented. Such atoms as the electronegative nitrogen and the electropositive phosphorus induce on phenyl *ipso* carbon atoms positive and negative charges, respectively, and indirectly affect charges on the other carbon atoms. This leads to elongation of the C<sub>*ipso*</sub>–C bond and to deformation of the α, β, γ, and δ bond angles. Figure 4 shows the corresponding charge densities on carbon atoms, calculated by the Mulliken

method for diphenylamine and diphenylphosphine (in parentheses), as well as the calculated C–C bond length in the C:<sup>2–7</sup> phenyl ring in diphenylamine. From these data it follows that the charge distribution in the C<sup>8</sup>...C<sup>13</sup> ring in diphenylamine is symmetric and adequate to that in phenylamine (the C<sup>9</sup>, C<sup>13</sup>, and C<sup>11</sup> atoms bear more negative charges than C<sup>10</sup> and C<sup>12</sup>). The charge distribution in the C<sup>2</sup>...C<sup>7</sup> ring is not so symmetric (the charges on C<sup>3</sup> and C<sup>7</sup> differ by –0.02 au). Similar pattern is observed in diphenylphosphine: The C<sup>2</sup>...C<sup>7</sup> ring is symmetric and C<sup>8</sup>...C<sup>13</sup> is asymmetric (the difference in the atomic charges attains –0.02 au). We explain the distortions in symmetric charge distribution in both phenyl rings to the deviation of the *l<sub>p</sub>*(NCC) torsion angles (*l<sub>p</sub>* is the lone electron pair on the N atom) from 90° and to the above-mentioned steric factors. Figure 4 also shows the C–C bond lengths in diphenylamine. There are no any correlations between the difference in the charges on adjacent carbon atoms that form a covalent bond and the length of this bond.

It is to be noted that the C–N bond in phenylamine

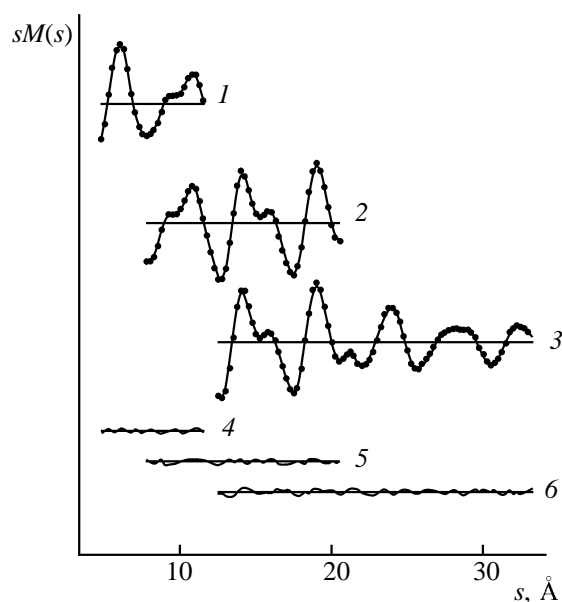


**Fig. 2.** (1, 2) Molecular intensity curves [(points) experiment and (solid line) calculation] and (3)  $\Delta sM(s) = sM(s)_{\text{exp}} - ksM(s)_{\text{calc}}$ .

(1,397 Å) is 0.002–0.003 Å shorter [28] than in diphenylamine. It will be remembered that the physical meaning of microwave  $r_z$  parameters and our electron diffraction  $r_a$  parameters is different. Phenylamine has a  $C_s$  conformation with H(N) atoms located on the same side of the phenyl ring plane. In this conformation, the  $\tau[l_p(\text{NCC})]$  torsion angles are 90°. The respective angles in diphenylamine are 60° and 62°, which does not exclude  $n-\pi$  interaction.

The structures of diphenylamine and diphenylphosphine differ from each other in the average bond angle at nitrogen (119°) and phosphorous (96°), as well as in that the C–N bond length in the former is strongly shortened (to 1.42 Å). It is  $n-\pi$  interaction which shortens the C–N bond in diphenylamine

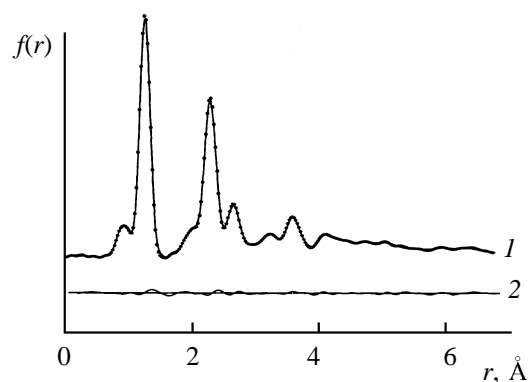


**Fig. 3.** (1) Radial distribution curve [(points) experiment and (solid line) calculation] and (2)  $\Delta f(r) = f(r)_{\text{exp}} - kf(r)_{\text{calc}}$ .

molecule and flattens its nitrogen pyramid. In phenylphosphines, the C–P bond length varies only slightly (1.83–1.84 Å [1–]). It is also important to note that the orientation of phenyl rings in phenylphosphines excludes  $n-\pi$  interaction.

Sasaki *et al.* reported electron diffraction data for triphenylamine [29]. The coordination of C–N bonds in the  $\text{NPh}_3$  fragment is close to planar [the molecule possesses  $C_3$  symmetry with the  $\angle\text{CNC}$  bond angle of 118° and  $\phi$  47(5)°]. Naturally, the referees failed to determine the C–N bond length reliably because of the strong correlation of this parameter with phenyl C–C bond lengths.

The electron diffraction study established that the diphenylamine molecule has an asymmetric structure. The coordination of the nitrogen atom is a flattened pyramid, the sum of bond angles around N is 353° and 357° (experiment and RHF/6-32G\*\* calculation, respectively). One may expect inversion of the N atom in the gas phase.

It is interesting to compare the geometries of the

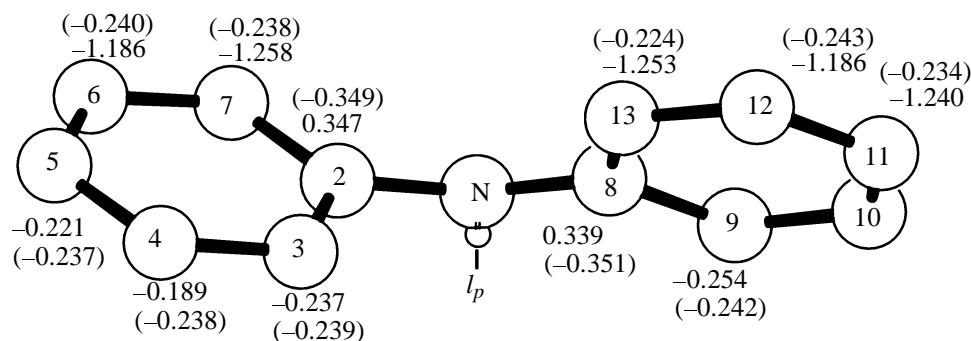


**Fig. 4.** Atomic charges, au, in diphenylamine and diphenylphosphine (in parentheses).



XPh<sub>2</sub> fragments in molecules of the XPh<sub>2</sub> series (X = O, S, NH, and OH). Diphenyl ether has an asymmetric structure with torsion angles around C–O bonds of 34° and 62° [30]. Experimental data for diphenyl sulfide SPh<sub>2</sub> are very limited [31]. The only determined parameters are C–S and C–C bond lengths and the CSC bond angle, whose values nicely fit calculation. Our RHF/6-31G\* and B3LYP/6-31G\* calculations suggest that the conformation of the molecule is of C<sub>2</sub> symmetry. Nevertheless, this problem has to be studied in more details by experiment and theory.

The crystal structure of diphenylamine was recently reported [32]. The unit cell contains eight independent asymmetric molecules (C<sub>1</sub> symmetry). The CNC bond angles vary in the range 127.3°–130.2°; the average value is 129.1(11)°. The sum of bond angles around the N atom is close to 359°. The average CC<sub>ipso</sub>C bond length is less 120° and equals 118.6°. The torsion angles around the N<sup>1</sup>–C<sup>2</sup> bonds (Fig. 1) are –457°, 297°, –367°, 487°, –357°, 497°, –457°, and 37° (on average, 177°). It is important to note the C<sub>ipso</sub>–C bonds in the phenyl rings are elongated (on average, to 1.395 Å), which agrees with theoretical calculations and experimental electron diffraction analysis of C<sub>1</sub> symmetry (Table 1). To conclude, the effective conformation of diphenylamine both in the gas and crystal phases is better described by an asymmetric model (C<sub>1</sub>).

## EXPERIMENTAL

The gas-phase electron diffraction patterns of diphenylamine were recorded on an EMR-100 electron diffraction unit with a cubic sector device, accelerating voltage 50 kV, nozzle temperature 50°C, nozzle-to-plate distances 179, 369, and 627 mm. The electron diffraction patterns were scanned on an MD-100 microdensitometer. The atomic scattering factors were taken from [33].

## ACKNOWLEDGMENTS

The work was financially supported in part by the Russian Foundation for Basic Research (project no. 03-03-04004).

## REFERENCES

1. Naumov, V.A., Tafipol'skii, M.A., and Shorokhov, D.Yu. *Zh. Obshch. Khim.*, 2001, vol. 71, no. 8, p. 1299.
2. Naumov, V.A., Tafipol'skii, M.A., Naumov, A.V., and Samdal, S. *Zh. Obshch. Khim.*, 2002, vol. 72, no. 12, p. 2002.
3. Naumov, V.A., Tafipol'skii, M.A., Naumov, A.V., and Samdal, S. *Zh. Obshch. Khim.*, 2003, vol. 73, no. 6, p. 948.
4. Zverev, V.V., Ermolaeva, L.V., and Kitaev, Yu.P., *Proceedings of Science conference of Institute of Organic and Physical Chemistry*, Kazan, 1971, p. 75.
5. Pankratov, A.N., Mushtakova, S.P., and Gribov, L.A., *Zh. Strukt. Khim.*, 1985, vol. 26, no. 5, p. 170.
6. Luzhkov, V.B. and Yakushchenko, T.N., *Zh. Strukt. Khim.*, 1990, vol. 31, no. 1, p. 30.
7. Sett, P., De, A.K., Chattopadhyay, S., and Mallick, P.K., *Chem. Phys.*, 2002, vol. 276, no. 2, p. 211.
8. Bredas, J.L., Quattrocchi, C., Libert, J., MacDiarmid, A.G., Ginder, J.M., and Epstein, A.J., *Phys. Rev. B*, 1991, vol. 44, no. 12, p. 121.
9. Boyle, A., *J. Mol. Struct. (Theochem)*, 1999, vol. 469, p. 15.
10. Ito, A., Ota, K., Yoshizawa, K., Tanaka, K., and Yamabe, T., *Chem. Phys. Lett.*, 1994, vol. 223, nos. 1–2, p. 27.
11. Choi, C.H. and Kertesz, M., *Macromolecules*, 1997, vol. 30, no. 3, p. 620.
12. Boogaarts, M.G.H., von Helden, G., and Meijer, G., *J. Chem. Phys.*, 1996, vol. 105, no. 19, p. 8556.
13. Tretiakov, I.V., and Cable, J.R., *J. Chem. Phys.*, 1997, vol. 107, no. 23, p. 9715.
14. Xiao, J.M., Gong, X.D., Chiu, Y.N., and Xiaob, H., *J. Mol. Struct. (Theochem)*, 1999, vol. 489, p. 151.
15. Budyka, M.F. and Zyubina, T.S., *Russ. J. Phys. Chem.*, 2000, vol. 74, no. 2, p. 347.
16. Becke, A.D., *J. Chem. Phys.*, 1993, vol. 98, no. 7, p. 5648.
17. Lee, C., Yang, W., and Parr, R.G., *Phys. Rev. B*, 1988, vol. 37, no. 8, p. 1123.
18. Frisch, M.J., Trucks, G.W., Schlegel, H.B., Scuseria, G.E., Robb, M.A., Cheeseman, J.R., Zakrzewski, V.G., Montgomery, J.A., Jr., Stratmann, R.E., Burant, J.C., Dapprich, S., Millam, J.M., Daniels, A.D., Kudin, K.N., Strain, M.C., Farkas, O., Tomasi, J., Barone, V., Cossi, M., Cammi, R., Mennucci, B., Pomelli, C., Adamo, C., Clifford, S., Ochterski, J., Petersson, G.A., Ayala, P.Y., Cui, Q., Morokuma, K., Salvador, P., Dannenberg, J.J., Malick, D.K., Rabuck, A.D., Raghavachari, K., Foresman, J.B., Cioslowski, J., Ortiz, J.V., Baboul, A.G., Stefanov, B.B., Liu, G., Liashenko, A., Piskorz, P., Komaromi, I., Gomperts, R., Martin, R.L., Fox, D.J., Keith, T., Al-Laham, M.A., Peng, C.Y., Nanayakkara, A., Challacombe, M., Gill, P.M.W., Johnson, B., Chen, W., Wong, M.W., Andres, J.L., Gonzalez, C., Head-Gordon, M., Replogle, E.S., and Pople, J.A., *GAUSSIAN*, Pittsburgh: Gaussian, 2001.

19. Dunning, T.H., Jr., *J. Chem. Phys.*, 1989, vol. 90, no. 2, p. 1007.
20. Srivastava, K.P. and Kumar, A., *Asian J. Chem.*, 2003, vol. 15, no. 2, p. 1140.
21. Kostic, R., Davidova, I.E., Gribov, L.A., and Rakovic, D., *J. Serb. Chem. Soc.*, 1990, vol. 55, no. 11, p. 617.
22. Cochet, M., Louarn, G., Quillard, S., Boyer, M. I., Buisson, J.P., and Lefrant, S., *J. Raman Spectrosc.*, 2000, vol. 31, p. 1029.
23. Mecke, R., *Longebucher. Infrared Spectra of Selected Chemical Compounds*, London: Heygen, 1965, vol. VI, p. 1257.
24. Mellier, A. and Brassy, C., *C. R. Acad. Sci., Sect. B*, 1973, vol. 276, no. 5, p. 177.
25. Sipachev, V.A., *J. Mol. Struct. (Theochem)*, 1985, vol. 121, p. 121.
26. Domenicano, A., *Stereochemical Applications of Gas-Phase Electron Diffraction*, Hargittai, I. and Hargittai, M., Eds., New York: VCH, 1988, pp. 281–324.
27. *Molecular Structures. Precise experimental methods*, Domenicano, A. and Hargittai, I., Eds, Moscow: Mir, 1997.
28. Lister, D.G., Tyler, J.K., Hong, J.H., and Larsen, N.W., *Struct.*, 1974, vol. 23, no. 2, p. 253.
29. Sasaki, Y., Kimura, K., and Kubo, M., *J. Chem. Phys.*, 1959, vol. 31, no.2, p. 477.
30. Naumov, V.A., Zaitdinova, R.N., Naumov, A.V., and Hagen, K. *Zh. Obshch. Khim.*, 2000, vol. 70, no. 2, p. 294.
31. Rozsondai, B., Moore, J.H., and Gregory, D.C., *Acta Chim. Acad. Sci.*, 1977, vol. 94, p. 321.
32. Rodriguez, M.A., and Bunge, S.D., *Acta Crystallogr., Sect. E*, 2003, vol. 59, no. 8, p. 1123.
33. Ross, A.W., Fink, M., and Hilderbrandt, R.L., *International Tables for X-Ray Crystallography*, Dordrecht: Kluwer, 1992, vol. C, p. 245.